Two-Dimensional Au and Au−Cu Alloy Nanocrystals with Orientation in (111) Plane Embedded in Glassy Silica Films‡

Goutam De† and C. N. R. Rao*

Chemistry and Physics of Materials Unit, Jawaharlal Nehru Centre for Advanced Scientific Research, Jakkur P.O., Bangalore 560 064, India

Received: August 22, 2003

Triangular Au and disk-shaped Au−Cu alloy nanocrystals have been generated in thin SiO_2 film matrixes, by sol−gel spin-coating followed by annealing at 800 °C in 10%H_2−90%Ar. Transmission electron microscope images confirm the shapes of the embedded nanocrystals. X-ray diffraction patterns reveal that the Au and Au−Cu nanocrystals have a (111) orientation. The disk-shaped alloy nanocrystals exhibit surface plasmon absorption at wavelengths intermediate between those of Au and Cu.

Metal nanocrystals embedded in appropriate glassy hosts are known to exhibit enhanced nonlinear optical properties, with a large intensity-dependent refractive index, which is related to the real part of the third-order susceptibility, $\chi^{(3)}$.[1] Such materials have potential optoelectronic applications in optical switching and optical limiting devices because of the ultrafast nonlinear response.[1,2] Optical properties of these composites are greatly influenced by the interface between the nanocrystals and the matrix.[3] Accordingly, the shape, size, and composition of the nanocrystals would play an important role in modulating the properties.[4−7] There is considerable interest today in synthesizing shape-controlled gold nanocrystals from solution.[8] A few other metal nanocrystals of different shapes, such as prism-shaped Ag,[9] disk-shaped Ag[10] and Co,[11] and triangular Ag,[12] have also been reported recently. For real applications, however, the nanocrystals have to be embedded in a suitable matrix which can withstand high-intensity laser light. Metal nanocrystals incorporated in thin films or glasses prepared by sol−gel,[1e,3c,7,13] ion-exchange,[14] ion-implantation,[1c,15] sputtering,[16] and glass fusion[17] are generally spherical in shape. Sol−gel-derived metal nanocrystals incorporated in SiO_2 films are known to exhibit high $\chi^{(3)}$ values with good reproducibility.[1e,f] In this communication, we report, for the first time, a sol−gel synthesis of highly oriented triangular Au nanoplates as well as of Au−Cu alloy nanodisks embedded in thin SiO_2 films, the alloy composition being in the range commonly employed for jewelry. Such shaped and oriented nanocrystals belonging to the quantum-size regime embedded in thin SiO_2 film might show interesting nonlinear optical responses.

Au and Au−Cu alloy nanocrystals embedded in silica hosts were prepared from sols starting with tetraethyl orthosilicate (TEOS), $HAuCl_4 \cdot 3H_2O$, $CuCl_2 \cdot 2H_2O$, *n*-propanol, *i*-butanol, and water, by the sol−gel spin coating technique. The compositions of the films are listed in Table 1. The molar ratio of the metal (M = Au, Au−Cu alloy, or Cu) to SiO_2 was kept constant in all the films, being 6 equivalent mol % M:94% SiO_2. The general method of preparation of the films was as follows. To a solution of TEOS in *n*-propanol (50% of the total) of the appropriate concentration, an aqueous-*n*-propanol solution containing $HAuCl_4 \cdot 3H_2O$ or/and $CuCl_2 \cdot H_2O$ was added under stirring, and the stirring continued for 2 h at 22 ± 2 °C. After this period, *i*-butanol was added and the sol was stirred for another 1 h. The total H_2O/TEOS molar ratio was maintained at 8. A catalytic amount of HCl was added (HCl/TEOS = 0.01) in the case of the pure Cu sol. The total equivalent SiO_2 and metal content of the sols was about 4.5 wt % in all cases. Films were deposited on clean silica glass slides (type II, Heraeus) or silicon wafers by spin-coating, employing a spinning rate of 1000−1500 rpm. The resulting films were dried at 75 °C in air followed by heat-treatment at 450 °C for 30 min to remove the organic matter. The films were heated in 10%H_2−90%Ar (gas flow was controlled by mass flow controller) at 700 °C for 1 h and then at 800 °C for 1 h. The film thickness, estimated by cross-sectional scanning electron microscopy (SEM), was in the 150−180 nm range. On annealing in air at 450 °C, Au metal nanocrystals were formed while Cu remained as an oxide.[7] Annealing in a 10%H_2/90%Ar atmosphere (450°−800 °C) reduced the Cu ions to metallic Cu and spontaneously formed Au−Cu alloys.

Powder X-ray diffraction (XRD) patterns of the thin film samples were recorded with a diffractometer operating at 40 kV and 30 mA using Ni-filtered Cu Kα radiation. In Figure 1, we show the XRD pattern of the SiO_2 film containing Au nanocrystals deposited on silica glass substrates. The pattern shows only the (111) Bragg reflection,[18] indicating a highly oriented growth of the Au nanocrystals. The (200) and (220) Bragg reflections are hardly visible (see inset of Figure 1). The XRD patterns of the films containing the Au−Cu alloy nanocrystals also show only the (111) reflection, indicating oriented growth (Figure 2). The *d*(111) value decreases with the increasing Cu content, showing the formation of good solid solutions (Table 1). Thus, in the case of Au_5Cu_1, the (111) reflection is 2.32 Å corresponding to $a = 0.4018$ nm while the *a* value calculated from Vegard's law is 0.4018 nm.[19,20] In Au_4Cu_2 and Au_3Cu_3, the *d* values are slightly higher, indicating a lower Cu concentration than indicated by the nominal composition (Table 1). So in the latter cases a very small amount of the Cu atoms do not form the alloy. The compositions of the alloys derived from the respective *d* values are listed in Table 1. It is

* Corresponding author. Phone: +91 80 8563075. Fax: +91 80 8462760. E-mail: cnrrao@jncasr.ac.in.

† Permanent address: Sol-Gel Division, Central Glass and Ceramic Research Institute, Jadavpur, Kolkata 700 032, India.

‡ This manuscript is in honor of Professor Henglein's 65th birthday.

10.1021/jp0310091 CCC: $25.00
Published on Web 11/14/2003

TABLE 1: Composition of the Films Obtained after Annealing at 800 °C for 1 h in 10%H_2/90%Ar

starting composition (mol Au/mol Cu/mol Si)	sample name	alloy composition (nominal)	lattice parameter (nm) obtained from XRD	calculated alloy composition using Vegard's law[19,20]
6:0:94	Au	Au	0.4079	Au
5:1:94	Au_5Cu_1	$Au_{0.833}Cu_{0.166}$	0.4018	$Au_{0.833}Cu_{0.166}$
4:2:94	Au_4Cu_2	$Au_{0.666}Cu_{0.333}$	0.3969	$Au_{0.71}Cu_{0.29}$
3:3:94	Au_3Cu_3	$Au_{0.5}Cu_{0.5}$	0.3939	$Au_{0.637}Cu_{0.363}$
0:6:94	Cu	Cu	0.3615	Cu

noteworthy that no tetragonally ordered Au−Cu phase (tetra-auricupride, $a = 0.3960$ nm, $c = 0.3670$ nm) occurs in Au_3Cu_3 ($Au_{0.5}Cu_{0.5}$), as commonly observed in Au−Cu alloys sequentially implanted in silica.[14a] The mean particle diameter calculated from the (111) reflections are Au = 42 nm, Au_5Cu_1 = 25 nm, Au_4Cu_2 = 18 nm, and Au_3Cu_3 = 14 nm, showing a decrease in size with increasing Cu concentration.

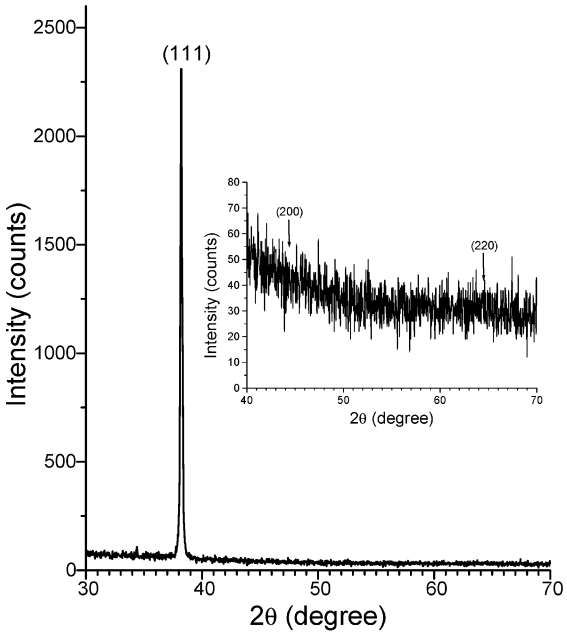

Figure 1. XRD pattern of Au nanocrystals embedded in SiO_2 thin film. Inset shows an expanded region (40−70° 2θ) of the XRD pattern.

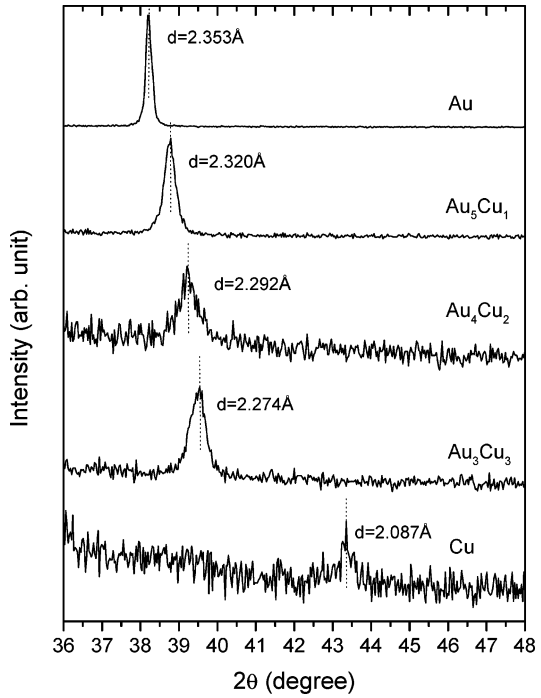

Figure 2. XRD patterns of nanocrystals of Au, Cu and Au−Cu alloys embedded in SiO_2 thin film matrixes.

A transmission electron microscope (TEM) image of the triangular Au nanocrystals is shown in Figure 3. The image (Figure 3a) shows the presence of platelike triangular nanocrystals, along with occasional hexagonal nanocrystals in the size range of 15−45 nm. Magnified views of the triangular and hexagonal nanocrystals can also be seen in Figure 3 marked as (b) and (c). As seen in figure the platelets are mostly triangular in shape, so it is expected that the triangular plates are formed first and, in some cases, excess local concentration of Au probably facilitates the formation of hexagonal shapes.[8b]

The TEM image of the $Au_{0.666}Cu_{0.333}$ (Au_4Cu_2) film is shown in Figure 4, to reveal two-dimensional flat nanocrystals in different size ranges (bigger ones of 10−25 nm diameter and smaller ones of 3−10 nm diameter). The magnified images (horizontal and tilted views marked A and B, respectively) are also shown in the figure to illustrate the disklike features. The contrast in the overlap region of the nanocrystals and the tilted view indicate that the nanodisks are rather thin (Figure 4). The selected area electron diffraction pattern, given in the inset of Figure 4, shows the presence of spots corresponding to a single

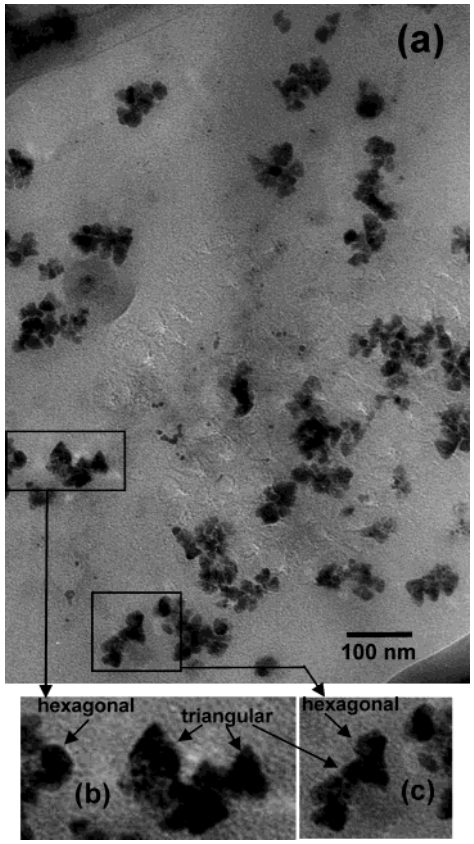

Figure 3. TEM image of an Au film showing (a) the presence of triangular and occasional hexagonal Au nanocrystals, (b) and (c) are the magnified view of the marked area of (a).

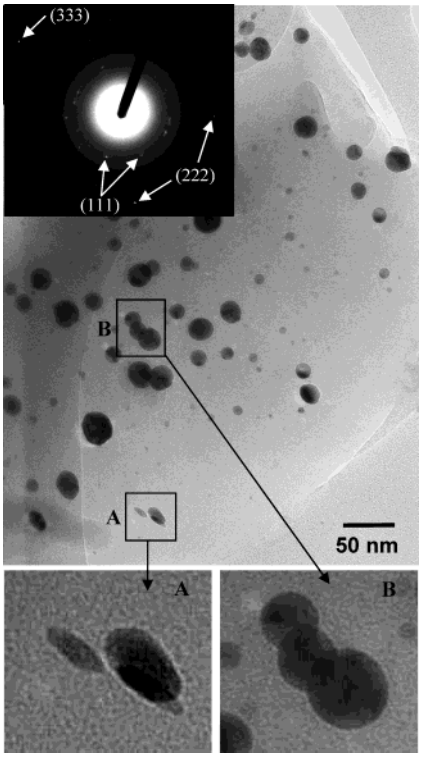

Figure 4. TEM image of a $Au_{0.666}Cu_{0.333}$ (Au_4Cu_2) film showing Au−Cu alloy nanodisks embedded in the SiO_2 thin film (inset shows the selected area electron diffraction). The portions marked A and B are shown in magnified form to illustrate the disklike features.

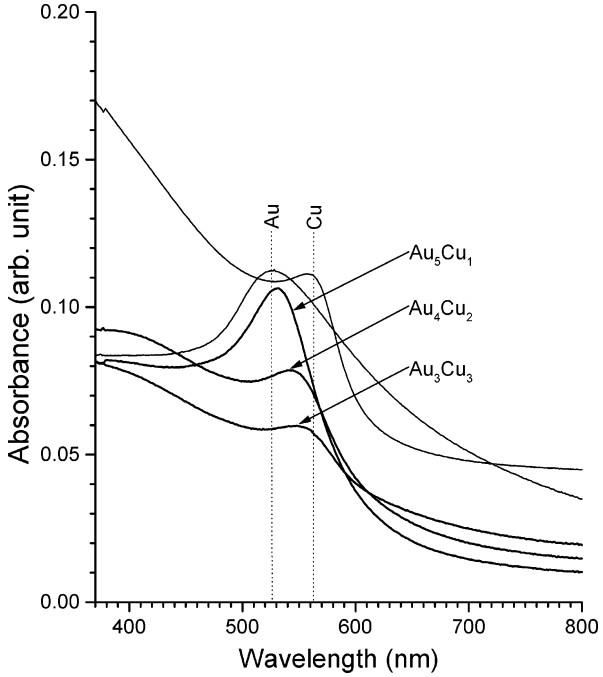

Figure 5. Optical absorption spectra of Au, Au−Cu alloys, and Cu nanocrystals embedded in SiO_2 thin film matrixes.

fcc phase with $a = 0.3955 \pm 0.001$ nm, close to the expected value (0.3951 nm) for the composition $Au_{0.666}Cu_{0.333}$. The a value of this alloy calculated from the (111) XRD reflection is 0.3969 nm and this small difference can arise if the bigger particles are slightly deficient in Cu. It may be pointed out here that we are first to notice formation of disk-shaped, oriented Au−Cu alloy nanoparticles in side thin SiO_2 film matrix. At this point of time, however it is not possible to predict why we obtain triangular/heaxagonal-shaped nanocrystals in the case of Au and disk-shaped nanocrystals in case of AuCu alloy.

Figure 5 shows the optical spectra of the films heated at 800 °C for 1 h in 10%H_2/90%Ar. The pure Au film shows a band at 526 nm with a broad tail extending toward higher wavelengths due to surface plasmon resonance (SPR). The pure Cu film shows a relatively sharp SPR band around 563 nm. The SPR band of well-dispersed spherical Au nanocrystals is generally sharp and appears around 520 nm. The broadening of this band at higher wavelengths (Figure 5) is due to the anisotropy of the triangular Au nanocrystals.[5,8a] The alloy films show SPR bands in the intermediate positions between those of Au and Cu. As the alloy nanocrystals are nearly circular in shape, with the particle size decreasing with increasing Cu concentration, their optical absorption in the higher wavelength region is not prominent as in the case of triangular Au nanocrystals. The progressive red shift of the SPR band of the alloy nanocrystals with increasing Cu content is consistent with the known behavior of Au−Cu and Ag−Au alloys.[4,7]

It may be pointed out here that although different geometrical shapes were obtained in cases of Au (triangular, hexagonal) and Au−Cu (circular disks) nanocrystals, they are all single crystals having *fcc* structure with their basal plane as the (111) plane. Such platelike structural features in the case of gold[5,8a−d,i] and other noble metal nanocrystals[9,10,12] obtained through nucleation and growth in solution have been found and Kossel-Stranski theory of face-selective growth of crystals has been used to explain the growth mechanism.[5,21] In this work, we notice for the first time that Au (mainly triangular) and Au−Cu (circular) nanoplates could be generated inside a glassy SiO_2 film matrix after heat treatment at 800 °C in 10%H_2/90%Ar gas atmosphere using a simple sol−gel approach without using any capping agent or surfactants in the sols. In this case, the nucleation and growth of flat nanocrystals occurred in the solid state, concurrently with the densification of SiO_2 films, and further study is therefore necessary to establish the growth mechanism.

In conclusion, a sol−gel synthesis of triangular Au nanoplates and of Au−Cu alloy nanodisks embedded in thin SiO_2 matrixes has been accomplished. The alloys possess the *fcc* structure, with the lattice parameter decreasing with Cu content. The flat Au and Au−Cu alloy nanocrystals exhibit (111) orientation. The plasmon band is red-shifted in the alloy nanocrystals.

Acknowledgment. This manuscript is in honor of Professor Henglein's 65th Birthday.

References and Notes

(1) Hache, H.; Ricard, D.; Flytzanis C. *J. Opt. Soc. Am.* **1986**, *B3*, 1647. (b) Flytzanis C.; Hache, F.; Klein, M. C.; Ricard, D.; Roussignol, Ph. *Prog. Opt.* **1991**, *29*, 321. (c) Gonella, F.; Mazzoldi, P. Metal Nanocluster Composite Glasses. In *Handbook of Nanostructured Materials and Nanotechnology*; Nalwa, H. S., Ed.; Academic Press: San Diego, 2000; Vol. 4, pp 81−158. (d) Del Fatti, N.; Vallee, F. *Appl. Phys.* **2001**, *B73*, 383. (e) De, G.; Tapfer, L.; Catalano, M.; Battaglin, G.; Caccavale, F.; Gonella, F.; Mazzoldi, P.; Haglund, R. F., Jr. *Appl. Phys. Lett.* **1996**, *68*, 3820. (f) Prem Kiran, P.; De, G.; Rao, D. N. In *Proceedings of the 6th International Conference on Optoelectronics, Fibre Optics and Photonics: 'Photonics 2002'*, TIFR: Mumbai, 2002, paper no. NLO P21.

(2) Sun, Y.-P.; Riggs, J. E.; Henbest, K. B.; Martin, R. B. *J. Nonlinear Opt. Phys. Mater.* **2000**, *9*, 481.

(3) Butcher, P. N.; Cotter, D. *The Elements of Nonlinear Optics*; Cambridge University Press: Cambridge, U.K., 1990. (b) Creighton, J. A.; Eadon, D. G. *J. Chem. Soc., Faraday Trans.* **1991**, *87*, 3881. (c) Gonella, F.; Mattei, G.; Mazzoldi, P.; Battaglin, G.; Quaranta, A.; De, G.; Montecchi, M. *Chem. Mater.* **1999**, *11*, 814. (d) Doremous, R. H. *Langmuir* **2002**, *18*, 2436.

(4) Kreibig, U.; Volmer, M. *Optical Properties of Metal Clusters*; Springer-Verlag: Berlin Heidelberg, 1995.

(5) Kirkland, A. I.; Jefferson, D. A.; Duff, D. G.; Edwards, P. P.; Gameson, I.; Johnson, B. F. G.; Smith, D. J. *Proc. Royal Soc. London A* **1993**, *440*, 589.

(6) Rao, C. N. R.; Kulkarni, G. U.; Thomas, P. J.; Edwards, P. P. *Chem. Eur. J.* **2002**, *8*, 29.

(7) De, G.; Mattei, G.; Mazzoldi, P.; Sada, C.; Battaglin, G.; Quaranta, A. *Chem. Mater.* **2000**, *12*, 2157.

(8) Milligan, W. O.; Morriss, R. H. *J. Am. Chem. Soc.* **1964**, *86*, 3461. (b) Zhou, Y.; Wang, C. Y.; Zhu, Y. R.; Chen, Z. Y. *Chem. Mater.* **1999**, *11*, 2310. (c) De, G.; Kundu, D. *Chem. Mater.* **2001**, *13*, 4239. (d) Malikova, N.; Pastoriza-Santos, I.; Scheirhorn, M.; Kotov, N. A. *Langmuir* **2002**, *18*, 3694. (e) Leontidis, E.; Kleitou, K.; Kyprianidou-Leodidou, T.; Bekiari, V.; Lianos, P. *Langmuir* **2002**, *18*, 3659. (f) Jana, N. R.; Gearheart, L.; Murphy, C. J. *J. Phys. Chem. B* **2001**, *105*, 4066. (g) El-Sayed, M. *Acc. Chem. Res*. **2001**, *34*, 257. (h) Swami, A.; Kumar, A.; Selvakannan, P. R.; Mandal, S.; Pasricha, R.; Sastry, M. *Chem. Mater*. **2003**, *15*, 17. (i) Prasad, B. L. V.; Stoeva, S. I.; Sorensen, C. M.; Klabunde, K. J. *Chem. Mater*. **2003**, *15*, 935.

(9) Jin, R.; Cao, Y.-W.; Mirkin, C. A.; Kelly, K. L.; Schatz, G. C.; Zheng, J. G. *Science* **2001**, *294*, 1901.

(10) Chen, S.; Fan, Z.; Carroll, D. L. *J. Phys. Chem. B* **2002**, *106*, 10777.

(11) Puntes, V. F.; Zanchet, D.; Erdonmez, C. K.; Alivisatos, A. P. *J. Am. Chem. Soc*. **2002**, *124*, 12874.

(12) Sun, Y.; Mayers B.; Xia, Y. *Nano Lett*. **2003**, *3*, 675.

(13) De, G. *J. Sol-Gel Sci. Technol*. **1998**, *11*, 289. (b) Epifani, M.; De, G.; Licciulli, A.; Vasanelli, L. *J. Mater. Chem*. **2001**, *11*, 3326. (c) Matsuoka, J.; Mizutani, R.; Kaneko, S.; Nasu, H.; Kamiya, K.; Kadono, K.; Sakaguchi, T.; Miya, M. *J. Ceram. Soc. Jpn.* **1993**, *101*, 53.

(14) Gonella, F.; Mattei, G.; Mazzoldi, P.; Spizzo, F.; Quaranta, A.; De, G. *Philos. Mag.* **1997**, *B76*, 621. (b) Caccavale, F.; De Marchi, G.; Gonella, F.; Mazzoldi, P.; Meneghini, C.; Quaranta, A.; Arnold, G. W.; Battaglin, G.; Mattei, G. *Nucl. Instrum. Methods* **1995**, *B96*, 382.

(15) Gonella, F.; Mattei, G.; Mazzoldi, P.; Sada, C.; Battaglin, G.; Cattaruzza, E. *Appl. Phys. Lett.* **1999**, *75*, 55. (b) Magruder, R. H., III; Osborne, D. H., Jr.; Zuhr, R. A.; *J. Non-Cryst. Solids* **1994**, *176*, 299.

(16) Akai, T.; Kadono, K.; Yamanaka, H.; Sakaguchi, T.; Miya, M.; Wakabayashi, H. *J. Ceram. Soc. Jpn.* **1993**, *101*, 105.

(17) Doremus, R.; Kao, S.; Garcia, R. *Appl. Opt.* **1992**, *31*, 5773.

(18) Leff, D. F.; Brandt, L.; Heath, J. R. *Langmuir* **1996**, *12*, 4723.

(19) The lattice parameter, a, of the Au−Cu *fcc* solid solution can be calculated from the modified Vegard's law: $a_{alloy} = xa_{Au} + (1 - x)a_{Cu} + 0.01198x(1 - x)$, where x is the Au fraction in the intermetallic alloy.

(20) Okamoto, H.; Chakrabarti, D. J.; Laughlin, D. E.; Massalski, T. B. In *Phase Diagrams of Binary Gold alloys;* Monograph Series of Alloy Phase Diagrams; ASM Internationals: Metals Park, OH, 1987.

(21) Bruche, B. *Kolloid-Z.* **1960**, *170*, 97.